JPET Fast Forward. Published on April 24, 2018 as DOI: 10.1124/jpet.118.248286
This article has not been copyedited and formatted. The final version may differ from this version.

Title Page

Title: Systematic modelling and design evaluation of unperturbed tumour dynamics in xenografts

Authors and affiliations:

Zinnia P Parra-Guillen, Victor Mangas-Sanjuan, Maria Garcia-Cremades, Iñaki F Troconiz, Gary Mo, Celine Pitou, Philip W Iversen, Johan E Wallin.

ZPP-G,VM-S,MG-C and IFT: Pharmacometrics & Systems Pharmacology Research Unit, Department of Pharmacy and Pharmaceutical Technology, School of Pharmacy and Nutrition, University of Navarra, Pamplona, Spain.

ZPP-G,VM-S,MG-C and IFT: IdiSNA, Navarra Institute for Health Research, Pamplona, Spain

GM, CP and JEW: Global PK/PD & Pharmacometrics, Eli Lilly and Company.

PWI: Lilly Research Laboratories, Eli Lilly and Company.

VM-S: Current affiliation: Department of Pharmacy and Pharmaceutical Technology and Parasitology, University of Valencia, Valencia, Spain; Molecular Recognition and Technological Development, Polytechnic University-University of Valencia, Valencia, Spain

MG-C: Current affiliation: Department of Bioengineering and Therapeutic Sciences, University of California, San Francisco, San Francisco, California, USA

ZPP-G and VM-S share first authorship

JPET Fast Forward. Published on April 24, 2018 as DOI: 10.1124/jpet.118.248286
This article has not been copyedited and formatted. The final version may differ from this version.

Running Title Page

Running title: Unperturbed tumour growth modelling and design

Corresponding author

Johan E Wallin

Gustav III Boulevard 42, P.O box 721. SE - 169 27 Solna. Sweden.

Phone: +46 8 737 88 69

Fax: +46 8 618 21 50

Email: wallinjo@lilly.com

Number of pages: 33

Number of figures: 5

Number of tables: 2

Number of references: 27

Abstract word count: 240

Introduction word count: 652

Discussion word count: 1349

Abbreviations: BIW: twice per week; FIM: Fisher information matrix; FOCEI: first order conditional estimation method; IAV: inter-animal variability; ISV: inter-study variability; l: length; NLME: nonlinear mixed effects; OFV: objective function value; PK: pharmacokinetics; PD: pharmacodynamics; Q2D: every two days; QW: every week; RSE: relative standard error; RUV: residual error estimate; SE: standard error; TGI: tumour growth inhibition; TV: tumour volume; TV_0: initial tumour volume; TVth : tumour threshold; VPC: visual predictive check; w:width; λ_0**:** exponential growth rate

JPET Fast Forward. Published on April 24, 2018 as DOI: 10.1124/jpet.118.248286
This article has not been copyedited and formatted. The final version may differ from this version.

constant; λ_1: linear growth rate constant; θ_i: individual model parameter; θ_{pop}: population parameter; ω^2: variance of the inter-individual variability; σ^2: variance of the residual variability; ψ: shape factor.

Recommended section: Drug Discovery and Translational Medicine

Abstract

Xenograft mice are largely used to evaluate the efficacy of oncological drugs during preclinical phases of drug discovery and development. Mathematical models provide a useful tool to quantitatively characterise tumour growth dynamics and also optimise upcoming experiments. To the best of our knowledge, this is the first report where unperturbed growth of a large set of tumour cell lines (n=28) has been systematically analysed using the model proposed by Simeoni in the context of non-linear mixed effect (NLME). Exponential growth was identified as the governing mechanism in the majority of the cell lines, with constant rate values ranging from 0.0204 to 0.203 day^{-1}. No common patterns could be observed across tumour types, highlighting the importance of combining information from different cell lines when evaluating drug activity. Overall, typical model parameters were precisely estimated using designs where tumour size measurements were taken every two days. Moreover, reducing the number of measurement to twice per week, or even once per week for cell lines with low growth rates, showed little impact on parameter precision. However, in order to accurately characterise parameter variability (i.e. relative standard errors below 50%), a sample size of at least 50 mice is needed. This work illustrates the feasibility to systematically apply NLME models to characterise tumour growth in drug discovery and development, and constitutes a valuable source of data to optimise experimental designs by providing an *a priori* sampling window and minimising the number of samples required.

Introduction

Drug discovery and development costs have been rising over the past years without translating into larger number of drugs approved by the regulatory agencies (Pharmaceutical Research and Manufacturers of America., 2016). This is especially relevant in the oncology area, where the attrition rates are among the highest (Hay *et al.*, 2014). One approach to reduce these alarming numbers is to look for strategies to better predict clinical trial outcome using early preclinical information (Zhang *et al.*, 2006).

Xenograft and syngeneic models are widely used in drug development to evaluate the antitumour effects of oncological compounds and guide the selection and development of drug candidates (Sausville and Burger, 2006; Ocana *et al.*, 2010). In these experiments, compounds exhibiting promising *in vitro* properties are tested on xenograft mouse experiments, typically across a small handful of different tumour cell lines. Success, is then measured in terms of achieved tumour regression/cure in the treatment group compared to the control group.

Many experimental variables such as cell line aggressiveness, tumour size at dosing time or dose intensity and frequency can significantly affect the evolution of tumour size over time, and consequently the outcome of these experiments in terms of observed shrinkage. Making an adequate choice of design can lead to more informative studies, with the additional benefit of reducing the number of animals, samples or repetition needed, and consequently reducing experimental costs, as recently illustrated by Lestini and colleagues (Lestini *et al.*, 2016). However, pharmacokinetic, pharmacodynamic and disease progression properties of the systems are rarely taken into account when designing xenograft experiments (Simeoni *et al.*, 2013).

On this regard, semi-mechanistic pharmacokinetic/pharmacodynamics (PKPD) analysis could constitute a powerful tool to integrate information from multiple experiments, and obtain design-independent model parameters that would enable then the *in silico* exploration and optimisation of potentially relevant scenarios. Non-linear mixed effect modelling (NLME) represents a suitable methodology in this context to quantitatively describe, not only the typical PKPD profile, but also to identify and quantify the different sources of variability (i.e across animals and experiments), thus allowing for better data description and understanding.

To characterise tumour size data from xenograft mice experiments, a model that considers two different processes in the natural course of tumour progression (exponential and linear) (Simeoni *et al.*, 2004) is commonly used. This model describes tumour growth dynamics in absence or presence of anticancer treatment and enables the computation of a threshold concentration (CT), such that if drug steady-state concentrations above that threshold are reached, the model will predict tumour shrinkage and eventually eradication. Indeed, Rochetti *et al.* (Rocchetti *et al.*, 2007) demonstrated a good correlation between CT and the active dose used in clinic for several marketed drugs, thus suggesting its potential for scaling efficacy from animal to man, further supporting the use of this preclinical model. To the best of our knowledge, NMLE methodology has been seldom used in the PKPD analysis of mice xenograft data, and if such, most of the studies focused on a limited number of cell lines or tumour types only (Bueno *et al.*, 2008; Parra-Guillen *et al.*, 2013; Tate *et al.*, 2014, 2016).

In this setting, the overall goal of our work was to illustrate how NLME modelling and optimal design theory can be systematically applied during the preclinical evaluation of new drug candidates to maximise the information that can be extracted from xenograft experiments, and enable its subsequent use in the design of future protocols. An accurate

description of the tumour dynamics in the absence of drug is a key step before characterising TGI drug effects. Therefore, unperturbed tumour growth data from a large set of tumour cell lines representing several cancer types was initially selected in this work to (i) characterise tumour growth dynamics in absence of active treatment (ii) evaluate the impact of study design and number of animals on the precision of parameter estimates, as well as (iii) the potential benefit of optimising the sampling time points.

Methods

Experimental data

Data from several experiments where tumour volume (TV) measurements from control mice were used. A total of 28 cell lines from 10 different tumour types were available for the analysis (see table 1 for an overview of the experimental data). Briefly, tumour cells were subcutaneously inoculated into athymic nude mice, weighing a mean of 23 g (16-32 g). Tumour size was measured with a calliper at regular times, and tumour volume was computed assuming tumour has an ovoid form: $(l \; x \; w^2)/2$ (Pierrillas *et al.*, 2016) where *l* is the length and *w* the width of the tumour in mm (l>w). Mice were sacrificed when measured tumour volume exceeded a pre-specified upper limit. All animal experiments were approved by the Eli Lilly and Company Institutional Animal Care and Use Committee.

Unperturbed tumour growth modelling

The model first proposed by Simeoni et al. (Simeoni *et al.*, 2004) was used to characterise the unperturbed tumour growth dynamics in all cell lines evaluated. Briefly, the model

JPET Fast Forward. Published on April 24, 2018 as DOI: 10.1124/jpet.118.248286
This article has not been copyedited and formatted. The final version may differ from this version.

describes an initial exponential increase in tumour volume followed by a linear growth, assuming no spontaneous tumour cell death and homogenous tumour cell behaviour:

$$\frac{dTV}{dt} = \frac{\lambda_0 \times TV}{\left[1 + \left(\frac{\lambda_0}{\lambda_1} \times TV\right)^{\psi}\right]^{\frac{1}{\psi}}} \qquad (eq.1)$$

TV is the tumour volume at any time after cell inoculation, and λ_0 and λ_1 are the first and zero order rate constants characterising the exponential and linear growth kinetics, respectively. The transition from exponential to linear growth occurs when TV reaches the value of the tumour threshold (TVth), which can be expressed as λ_1/λ_0. ψ is fixed to the value of 20, ensuring a rapid transition between the two different growth rates once TV reaches TVth. The initial condition of the system is given by TV_0, defined as the tumour volume immediately after tumour cell inoculation.

Nonlinear mixed effect modelling was used to analyse the data. The first order conditional estimation method with interaction (FOCEI) algorithm implemented in NONMEM 7.3 (Icon Development Solutions, Ellicott City, MD, USA) was selected.

During the analysis, the typical population parameters TV_0, λ_0, and λ_1 were estimated. Inter-animal (IAV) and inter-study variability (ISV) were explored on the three estimated typical parameters assuming a lognormal distribution of the individual parameters:

$$\theta_i = \theta_{pop} \times \exp(\eta_i) \qquad (eq.2)$$

where θ_i is the individual model parameter of mouse *i*, θ_{pop} the population parameter (i.e. TV_0, λ_0, or λ_1) and η_i the associated random effect of mouse *i* obtained from a normal distribution with mean 0 and estimated variance (ω^2).

JPET Fast Forward. Published on April 24, 2018 as DOI: 10.1124/jpet.118.248286
This article has not been copyedited and formatted. The final version may differ from this version.

TV data were logarithmically transformed for the analysis, and residual variability (accounting for the discrepancy between individual predictions and observations) was described using an additive error model on the logarithmic scale:

$$\log(TV_{i,j}) = \log(f(\Theta_i, t_j)) + \varepsilon_{i,j} \qquad (eq.3)$$

where $TV_{i,j}$ represents the tumour volume observations for the i^{th} animal at the j^{th} measurement time, $f(\Theta_i, t_j)$, corresponds to the predicted TV for mouse i^{th} at time j^{th} resulting from the vector of the i^{th} individual parameters Θ_i related as shown in eq. 1, and ε is the difference between the logarithm of the individual observed and predicted TV. The set of εs are independent between them and corresponds to a random variable mean 0 and estimated variance (σ^2).

Upper welfare limits for tumour size were not available for all the different studies, neither the reasons for drop-outs. Therefore, no censoring or drop-out model was considered in the analysis

Model selection and evaluation

Different statistical models (i.e. IAV parameters, ISV parameters and correlation between individual parameters) were explored and compared in terms of minimum value of the objective function (OFV) provided by NONMEM (approximately -2 log likelihood), precision of parameter estimates when obtained and goodness of fit. A decrease in OFV of 3.84 between two nested models was considered significant at 5% level.

Model performance was evaluated using the simulation-based diagnostics visual predictive checks (VPC) generated with PsN version 4 (Lindbom *et al.*, 2005) and Xpose4 R package (Jonsson and Karlsson, 1999). For each cell line, one thousand studies with the same design characteristics as the original experiments were simulated. For each simulated scenario (tumour cell line) and measurement interval (or bin) the 2.5th, 50th,

and 97.5th percentiles of the simulated TV values were calculated, then the 95% confidence intervals of the above mentioned predicted percentiles were obtained and presented graphically together with the 2.5^{th}, 50^{th}, and 97.5^{th} percentiles of the raw data.

Design evaluation and optimisation

According to the Cramer-Rao inequality, the inverse of the Fisher information matrix (FIM) is the lower bound of the variance-covariance matrix of any unbiased parameter estimate (Radhakrishna Rao, 1945; Cramér, 1946). Therefore, the SE can be obtained from the square root of the diagonal elements of the inverse of the FIM. The optimal design R package POPED (Foracchia *et al.*, 2004) was used to compute parameter precision - i.e relative residual errors (RSE) calculated as the ratio between standard errors (SE) and parameter estimates- obtained for the different studied cell lines, given the selected model, the final set of parameter estimates and an experimental design.

Parameter precision was evaluated under 3 distinct sampling schemas: (i) the standard schema of TV measurements taken every two days (Q2D), (ii) samples taken twice per week (BIW, i.e. two samples per week on day 1 and 4) or (iii) once per week (QW, i.e. one sample per week on day 1). For all the evaluations, the original number of mice per study (ranging from 7 to 287) and the sampling window (see Table 1) were kept unchanged. Note that although the selected acronyms commonly refer to the frequency of dose administration, in this context we used them to indicate the frequency at which TV measurements were taken. RSE obtained for the different model parameters across cell lines and evaluated sampling designs were analysed.

In a second step, the sampling times were optimised assuming 8 samples in all cases and allowing only for one tumour size sample per day. The study duration and the number of

animals were not optimised, i.e. original designs were used. The Adaptive Random Search methods implemented in POPED was used for the optimisation step.

Results

Unperturbed tumour growth

The unperturbed tumour growth model proposed by Simeoni *et al.* (Simeoni *et al.*, 2004) provided a good description of the data for all tumour cell lines, as illustrated in figure 1 for the case of lung cancer cell lines and in supplementary figure 1 for the rest of tumour cell lines.

Parameter estimates can be found in table 2. The estimates of the zero order rate constant [reflecting the linear tumour growth (λ_1)] ranged from 2.58 to 464 mm^3/day. With respect to λ_0, accounting for the exponential growth, and TV_0, the corresponding ranges were much smaller varying from 0.0204 to 0.203 day^{-1} and from 16 to 148 mm^3, respectively. Only for the case of the MB231, the estimate of λ_0 had to be fixed to a high value of 0.5 day^{-1}, indicating that only linear growth was observed in the measurable range (TV_{TH} of 5 mm^3).

IAV on λ_0 and/or TV_0 parameters was identified in all tumour cell lines, with a low to moderate magnitude ranging from 8 to 70 %, and 12 to 61 %, respectively. IAV in the λ_1 parameter could be estimated only in 10 out of 28 cell lines, with values ranging from 42 to 88 % (Fig.2A). This is due to the fact that for most cell lines little information was available over TV_{TH} –marking the shift from exponential to linear growth-, limiting thus the identification of IAV variability in λ_1. Correlation between individual parameters was explored during the modelling process and found significant only for A549 cell line (Table 2).

There were no relevant relationships between the magnitude of the different variability parameters and its typical estimate or the experimental size (Fig. 2B). Inclusion of inter-study variability did not show significance for the case of lung and melanoma cell lines, for which large number of studies were available ($p>0.05$).

Design evaluation and optimisation

POPED was used to evaluate the adequacy of the original experimental designs to precisely estimate all model parameters. In general, good precision (RSE below 10% in average) was obtained for the typical parameters when samples were measured every two days (Supplementary Tables 1-3 and Fig. 3A). The largest imprecision was detected on the linear growth rate (λ_1) for those tumours with a large tumour threshold (TV_{TH}). On the other hand, larger RSEs were observed for the variability parameters (Fig. 3A). Precision of the IAV parameters was highly dependent on the number of experimental mice (Fig. 4), regardless of the sampling schema evaluated. For a standard experimental size of 8-10 mice, RSEs between 50-60% would be observed. This clear trend was not significant for typical parameters and was independent on the value of IAV precision.

Similarly, the influence of reducing the number of sampling time measurements on parameter precision was evaluated. The BIW sampling schema (i.e. two samples per week) showed little impact on parameter precision, with a mean absolute loss <5% and a relative loss <25% for all parameters, except for residual error estimate (RUV) (Fig.3B). Further reducing to one sample per week (i.e. QW) worsened the precision of the typical parameter estimates, showing a mean absolute and relative loss >10%, but also more heterogeneous results (Fig.3B) highly dependent on the rate of tumour growth. This loss was less pronounced for the variability parameters, especially for λ_0.

Optimising the sampling times assuming a design of 8 samples per study provided results similar to assuming a fixed BIW schema (Fig. 3B). A wide range of sampling times, depending on the individual cell growth kinetics were observed (Supplementary Figure 2). However, in most of the cases clusters of sampling points around the initial, the tumour threshold (TVth, when relevant) and the latest possible collection sampling time were observed, as illustrated for 3 cell lines in figure 5.

Discussion

Although there is an on-going discussion on the capability of xenograft mouse models to generate meaningful data for human extrapolations, they are frequently used to evaluate the efficacy of anticancer drugs early in discovery and development. To overcome some of the limitations of these approaches, mathematical models have been proposed as a tool to derive meaningful parameters independent of the experimental settings, that can be later used to optimise upcoming experiments or guide dose rationale in humans (Simeoni *et al.*, 2013).

In this work, tumour growth dynamics of several tumour cell lines representing different tumour types were modelled in absence of drug using the model proposed by Simeoni *et al.* (Simeoni *et al.*, 2004). This model was selected as common structure to systematically analyse our data given its flexibility and proven capability to characterise tumour growth data from different xenograft mouse experiments, as supported by its extended literature use. This work adds to previous efforts characterising tumour growth dynamics with a common model (Wong *et al.*, 2012; Delgado-SanMartin *et al.*, 2015), and represents the first report where non-linear mixed effect modelling and optimal design techniques have been undertaken to quantitatively evaluate a large set of tumour cell lines.

The model proposed by Simeoni et al., (1) allowed for an adequate description of the unperturbed tumour growth under the different scenarios analysed. Obtained exponential growth rates (λ_0) were in good agreement with published estimates available for some cell lines (Simeoni *et al.*, 2004; Rocchetti *et al.*, 2005, 2007; Haddish-Berhane *et al.*, 2013; Terranova *et al.*, 2013; Tate *et al.*, 2014, 2016). It should be highlighted that in some cases, data did not fully support the two mechanisms of tumour growth. In those situations, model structure could have been simplified to consider just linear or exponential growth observing little impact on the rest of parameter estimates, as was done for the case of MB211. The maximum tumour burden allowed or drop-out information was not available and therefore not included in the analysis. This could have potentially induced some parameter estimation bias, especially for λ_1 (Martin *et al.*, 2016; Pierrillas *et al.*, 2016). However, given the large tumour size values observed in our experiments, the large number of mice available for some studies, and the lack of obvious trends or misspecifications observed for the larger tumour size predictions (Figure 1 and Supplementary Figure 1), we believe that considering the upper welfare limit in the analysis would have had little impact.

Given the availability of several independent experiments for same cell line, inclusion of inter-study variability in addition to inter-animal variability was explored. Inter-study variability did not provide further explanation of parameter variability, supporting study reproducibility. This work provides therefore valuable information to anticipate the dynamics of tumour growth in xenograft mice and support experimental design.

Dynamics of tumour growth in absence of drug treatment varied widely across the 28 different cell lines. The lower growth rate values were observed for the renal tumour type. However, no additional common patterns could be detected across cell lines for the same type of tumour. Indeed, a large range of tumour growth rate values was observed for lung cancer cells lines. This variability observed across cell lines suggests that information

from multiple cell lines obtained during pre-clinical studies should be integrated to improve extrapolation of results to clinical setting, rather than relying on single cell line experiments. Similar results have been recently illustrated by García-Cremades *et al.* for ovarian and pancreatic cancer (Garcia-Cremades *et al.*, 2016). A natural extension of this work would be to collect genetic, mutation and tumour histology information of the different cell lines and perform a bioinformatic analysis to identify (if any) common patterns that could account for similarities and differences in growth rates across the different cell types. This information could be potentially used to anticipate growth dynamics of new cell types based on their genetic signature.

An essential aspect when interpreting modelling results is the reliability of the obtained parameter estimates, i.e. large parameter imprecision translates into high uncertainty in model predictions and therefore limited extrapolation capability. On this regard, the experimental design plays an essential role on parameter estimates (al-Banna *et al.*, 1990). Measuring tumour size twice per week (BIW) allowed for a precise estimation of typical model parameters in all evaluated cell lines, with a small precision loss compared to measuring every two days. However, further reducing the sampling schema to once per week (QW) showed a less consistent impact on precision loss, with lower impact on parameter precision in slow growing tumours compare to fast growing tumours. Results from this evaluation design exercise showed that the underlying properties of the cell line can be used to guide experimental design, in terms of sampling intensity and/or size of the experiment.

Among the unperturbed growth model parameters, special attention should be paid to λ_0, as this parameter is potentially utilised to predict the target human exposure of a candidate drug (Rocchetti *et al.*, 2007). Except for Mia Paca-2 cell line, where linear rather than exponential growth was the predominant mechanism, RSE of λ_0 was always below the 20%, regardless of the experimental setting (e.g. number of mice, parameter value) and sampling schema. These observations illustrate the adequacy of NLME approach to

precisely characterise and rank the typical exponential growth rate of the different cell lines. Another important aspect to consider, due to its impact on the confidence interval around the predicted tumour size profiles, is the precision of the estimated variability. Accuracy of IAV parameters was largely driven by the number of mice, rather than the sampling schema or the IAV magnitude, with approximately 50 animals required for RSE<50%. NLME represents a suitable approach to achieve such large sample size, since it enables the integration of data from multiple experiments and even control and treatment groups. In addition, parameters reported in this manuscript, could be used as prior information, to further reduce the size of control groups.

One step further in the application of optimal design theory is the optimisation of the selected sampling times, i.e. identifying those times that, given a model structure and some design constrains, provide the maximum possible information for the estimation of the different model parameters. Optimal design strategies applied to xenograft data have been recently proposed by Lestini et al. (Lestini *et al.*, 2016). Their results showed how optimal sampling schemas can improve the information obtained from experimental data and highlight the importance of early and late sampling for an adequate parameter characterisation. Comparable results were obtained in our analysis of control groups, identifying clusters of points at early sampling times (informed about TV_0), late sampling times (informed about the linear growth) or TV_{TH} (exponential and linear growths) (Fig.5 and Fig.S2). Similarities or differences between optimal times across cell types are therefore explained by the similarities or differences in their growth behaviour.

Nonetheless, evaluation of experimental designs that can be systematically applied under different conditions might be of more relevance than optimising the sampling times for each of the cell lines, especially given the low cost and time consumption for obtaining

tumour size measurements, and the convenience of standard designs in terms of experimental organisation.

In conclusion, a common structure based on the model proposed by Simeoni *et al*. characterised well the typical and dispersion tendencies of the longitudinal tumour volume data obtained from a wide range of tumour cell lines providing a robust and general platform to (i) quantify and compare tumour growth and possibly (ii) design future treatment experiments based on information from treated groups, *in vitro* data regarding drug potency and drug pharmacokinetics. Experimental designs measuring tumour size twice weekly, or even once a week for slow growing tumours, are sufficient for an accurate characterisation of the tumour growth dynamics. However, analysis of pooled experiments to increase the number of mice are required for an adequate quantification of variability. The approach presented can be easily extrapolated also to drug studies, where modelling and simulation together with design optimisation is anticipated to have a more relevant role given the greater experimental studies alternatives, e.g. dose level, dose intensity or group size.

Acknowledgments

The authors would like to thank Andrew Hooker, France Mentré and Giulia Lestini for the support received in the use of optimal design theory.

Authorship contribution

Participated in research design: Parra-Guillen, Mangas-Sanjuan, Garcia-Cremades, Troconiz, Mo, Pitou, Iversen, and Wallin

Conducted experiments: Parra-Guillen, Mangas-Sanjuan, Garcia-Cremades, Troconiz, Mo, Pitou, Iversen, and Wallin

Performed data analysis: Parra-Guillen, Mangas-Sanjuan, Garcia-Cremades, Troconiz, Mo, Pitou, Iversen, and Wallin

Wrote or contributed to the writing of the manuscript: Parra-Guillen, Mangas-Sanjuan, Garcia-Cremades, Troconiz, Mo, Pitou, Iversen, and Wallin

Reference

al-Banna MK, Kelman AW, and Whiting B (1990) Experimental design and efficient parameter estimation in population pharmacokinetics. *J Pharmacokinet Biopharm* **18**:347–60.

Bueno L, de Alwis DP, Pitou C, Yingling J, Lahn M, Glatt S, and Trocóniz IF (2008) Semi-mechanistic modelling of the tumour growth inhibitory effects of LY2157299, a new type I receptor TGF-β kinase antagonist, in mice. *Eur J Cancer* **44**:142–150.

Cramér H (1946) *Methods of mathematical statistics*. Princeton University Press, Princeton

Delgado-SanMartin JA, Hare JI, de Moura APS, and Yates JWT (2015) Oxygen-Driven Tumour Growth Model: A Pathology-Relevant Mathematical Approach. *PLoS Comput Biol* **11**:1–20.

Foracchia M, Hooker A, Vicini P, and Ruggeri A (2004) poped, a software for optimal experiment design in population kinetics. *Comput Methods Programs Biomed* **74**:29–46.

Garcia-Cremades M, Pitou C, Iversen PW, and Troconiz IF (2016) A comparison of different model-based approaches to scale preclinical to clinical tumour growth inhibition in gemcitabine-treated pancreatic cancer, in *PAGE 25 (2016) Abstr 5704, (2016) [www.page-meeting.org/?abstract=5704]*.

Haddish-Berhane N, Shah DK, Dangshe M, Leal M, Gerber H-P, Sapra P, Barton HA, and Betts AM (2013) On translation of antibody drug conjugates efficacy from mouse experimental tumors to the clinic: a PK/PD approach. *J Pharmacokinet Pharmacodyn* **40**:557–571.

Hay M, Thomas DW, Craighead JL, Economides C, and Rosenthal J (2014) Clinical development success rates for investigational drugs. *Nat Biotechnol* **32**:40–51.

Jonsson EN, and Karlsson MO (1999) Xpose--an S-PLUS based population pharmacokinetic/pharmacodynamic model building aid for NONMEM. *Comput Methods Programs Biomed* **58**:51–64.

Lestini G, Mentré F, and Magni P (2016) Optimal Design for Informative Protocols in Xenograft Tumor Growth Inhibition Experiments in Mice. *AAPS J* **18**:1–11.

Lindbom L, Pihlgren P, and Jonsson N (2005) PsN-Toolkit—A collection of computer intensive statistical methods for non-linear mixed effect modeling using NONMEM. *Comput Methods Programs Biomed* **79**:241–257.

Martin EC, Aarons L, and Yates JWT (2016) Accounting for dropout in xenografted tumour efficacy studies: integrated endpoint analysis, reduced bias and better use of animals. *Cancer Chemother Pharmacol* **78**:131–41, Springer.

Ocana A, Pandiella A, Siu LL, and Tannock IF (2010) Preclinical development of molecular-targeted agents for cancer. *Nat Rev Clin Oncol* **8**:200–209.

Parra-Guillen ZP, Berraondo P, Ribba B, and Trocóniz IF (2013) Modeling tumor response after combined administration of different immune-stimulatory agents. *J Pharmacol Exp Ther* **346**:432–442.

Pharmaceutical Research and Manufacturers of America. (2016) *2016 Biopharmaceutical research industry profile. http://phrma-docs.phrma.org/sites/default/files/pdf/biopharmaceutical-industry-profile.pdf*.

Pierrillas PB, Tod M, Amiel M, Chenel M, and Henin E (2016) Improvement of

Parameter Estimations in Tumor Growth Inhibition Models on Xenografted Animals: a Novel Method to Handle the Interval Censoring Caused by Measurement of Smaller Tumors. *AAPS J* **18**:404–415.

Radhakrishna Rao C (1945) Information and the Accuracy Attainable in the Estimation of Statistical Parameters. *Bull Calcutta Math Soc* **37**:81–91.

Rocchetti M, Poggesi I, Germani M, Fiorentini F, Pellizzoni C, Zugnoni P, Pesenti E, Simeoni M, and De Nicolao G (2005) A pharmacokinetic-pharmacodynamic model for predicting tumour growth inhibition in mice: A useful tool in oncology drug development. *Basic Clin Pharmacol Toxicol* **96**:265–268.

Rocchetti M, Simeoni M, Pesenti E, De Nicolao G, and Poggesi I (2007) Predicting the active doses in humans from animal studies: A novel approach in oncology. *Eur J Cancer* **43**:1862–1868.

Sausville EA, and Burger AM (2006) Contributions of Human Tumor Xenografts to Anticancer Drug Development. *Cancer Res* **66**:3351–3354.

Simeoni M, De Nicolao G, Magni P, Rocchetti M, and Poggesi I (2013) Modeling of human tumor xenografts and dose rationale in oncology. *Drug Discov Today Technol* **10**:e365–e372.

Simeoni M, Magni P, Cammia C, De Nicolao G, Croci V, Pesenti E, Germani M, Poggesi I, and Rocchetti M (2004) Predictive Pharmacokinetic-Pharmacodynamic Modeling of Tumor Growth Kinetics in Xenograft Models after Administration of Anticancer Agents. *Cancer Res* **64**:1094–1101.

Tate SC, Burke TF, Hartman D, Kulanthaivel P, Beckmann RP, and Cronier DM (2016) Optimising the combination dosing strategy of abemaciclib and vemurafenib in

BRAF-mutated melanoma xenograft tumours. *Br J Cancer* **114**:669–679.

Tate SC, Cai S, Ajamie RT, Burke T, Beckmann RP, Chan EM, De Dios A, Wishart GN, Gelbert LM, and Cronier DM (2014) Semi-mechanistic pharmacokinetic/pharmacodynamic modeling of the antitumor activity of LY2835219, a new cyclin-dependent kinase 4/6 inhibitor, in mice bearing human tumor xenografts. *Clin Cancer Res* **20**:3763–3774.

Terranova N, Germani M, Del Bene F, and Magni P (2013) A predictive pharmacokinetic–pharmacodynamic model of tumor growth kinetics in xenograft mice after administration of anticancer agents given in combination. *Cancer Chemother Pharmacol* **72**:471–482.

Wong H, Choo EF, Alicke B, Ding X, La H, McNamara E, Theil F-P, Tibbitts J, Friedman LS, and Hop CECA (2012) Antitumor Activity of Targeted and Cytotoxic Agents in Murine Subcutaneous Tumor Models Correlates with Clinical Response. *Clin Cancer Res* **18**:3846–3855, AACR.

Zhang L, Sinha V, Forgue ST, Callies S, Ni L, Peck R, and Allerheiligen SRB (2006) Model-Based Drug Development: The Road to Quantitative Pharmacology. *J Pharmacokinet Pharmacodyn* **33**:369–393.

Footnotes

At the time the research was performed, ZPP-G, VM-S, MG-C and IFT received research funding from Eli Lilly & Company.

Legend for Figures

Figure 1: Visual predictive checks of the unperturbed tumour growth model corresponding to lung tumour cell lines. Lines represent the 2.5th (dashed), 50th (solid) and 97.5th (dashed) percentiles of raw data. Grey areas correspond to the 95% confidence interval of the 2.5th, 50th and 97.5th percentiles computed from 1000 simulated studies. Black lower marks indicate the used binning intervals for plotting.

Figure 2: (A) Graphical representation of the parameter estimates for the different tumour cells lines categorised by number of studies available and the associated variability magnitude. (B) Relation between the estimate of the different inter-animal variability (IAV) and the number of mice included in the analysis of each cell line.

Figure 3: (A) Boxplot of the relative standard errors (RSE) for the structural and variability model parameters (parameter definition provided in the Methods and Material section) of the different cell lines assuming samples taken every two days (Q2D). (B) Boxplot representing the predicted precision when evaluating the sampling designs twice per week (BIW), once per week (QW) or the optimised sampling schema (OPT8) with respect to the Q2D reference design. The box represents the interquartile range (IQR) and the whiskers expand up to 1.5 times the IQR range. Dots represent outliers.

Figure 4: Relative standard error of the typical (upper panels) or inter-animal variability (IAV) (lower panels) model parameters versus the number of mice included in the analysis of the different cell lines. Q2D: tumour size samples taken every two days. BIW: tumour size samples taken twice per week. QW: tumour size samples taken every week.

Figure 5: Tumour volume profiles for 3 selected cell lines. Lines represent model predictions and dots represent the optimised sampling times.

Tables

Table 1: Summary of the experimental data available for each of the tumour cell lines

Tumour	Cell	Nº of studies	Nº of mice	Nº of samples	T_{MIN} (days)	T_{MAX} (days)
Breast	MB-231	1	45	423	11	45
Colon	COLO205	5	85	668	6	120
	HCT116	1	10	25	7	17
Glioblastoma	U-87 MG	3	100	382	7	63
Leukemia	MV411	2	33	388	7	73
Lung	A549	2	33	389	7	69
	Calu-6	2	25	288	7	59
	DMS53	1	6	120	7	98
	H1650	2	21	277	7	62
	H1975	3	61	361	7	41
	H2122	8	92	763	7	50
	H358	1	8	160	10	88
	H441	17	287	3391	3	98
	H460	1	13	109	8	47
	HCC827	1	8	99	10	55
Lymphoma	JEKO-1	4	31	312	7	46
	OCI-LY-19	2	38	178	7	32
	WILL-2	1	24	80	7	23
Melanoma	A2058	2	20	177	7	35
	A375	8	104	840	3	69
	GAK	2	15	181	8	56
	SK-MEL-30	2	24	229	0	45
Ovarian	A2780	1	8	68	8	37
	SKVO-3	1	8	104	7	47
Pancreas	MIA PaCa-2	1	8	64	11	41
Renal	786-o	4	52	740	6	76
	ACHN	3	50	604	7	60
	Caki-1	1	13	116	13	51

Tmin: Time at which tumour could start to be measured.
Tmax: Latest sampling time available in the experiment

Table 2: Model parameter estimates corresponding to all the tumour cell lines analysed

Tumour Line	Cell Line	Parameters							
		λ_0 [day^{-1}]	λ_1 [mm^3/day]	TV_0 [mm^3]	TV_{TH} [mm^3]	IAV λ_0 [CV%]	IAV λ_1 [CV%]	IAV W_0 [CV%]	RUV [log mm^3]
Lung	A549	0.051	58.5	48.2	1150	19.8[a]		29.5[a]	0.205
	H460	0.104	237	71.3	2280	25.2		25.9	0.148
	HCC827	0.100	35.1	21.8	351	16.9			0.194
	Calu-6	0.0875	126	49.9	1440	27.2	53.2	12.6	0.147
	DMS53	0.0438	27.6	16.0	630	11.0			0.316
	H1650	0.0575	48.0	50.6	835	20.1		12.8	0.201
	H1975	0.104	188	46.3	1810	14.8			0.202
	H358	0.0204	115	88.6	5640	30.0			0.129
	H441	0.0342	75.0	69.6	2190	68.6		40.1	0.223
	H2122	0.103	42.6	60.2	414	20.4	45.1	23.0	0.151
Renal	ACHN	0.0249	12.8	123	514	68.7	42.5	19.7	0.162
	CAKI-1	0.0265	64.2	102	2420			14.3	0.239
	786-o	0.0489	29.5	82.4	603	22.4	67.7	26.4	0.176
Melanoma	A2058	0.129	55.9	64.7	433	8.20	39.6		0.154
	A375	0.0948	101	69.3	1070	39.8	67.2	36.3	0.193
	GAK	0.0277	19.0	88.8	686	45.5		17.6	0.191
	SK-MEL-30	0.0640	84.8	148	1330	45.9		23.7	0.200
Lymphoma	JEKO-1	0.0825	217	62.9	2630	10.5		19.3	0.284
	OCI-LY-19	0.138	464	30.0	3360	9.70			0.320
	WILL-2	0.203	352	25.3	1730			28.0	0.263
Colon	COLO205	0.106	31.9	65.6	301	25.1	88.1	61.5	0.211
	HCT116	0.121	176	67.5	1460	19.3			0.409
Glioblastoma	U-87-MG	0.0547	51.9	80.4	949	38.9		29.0	0.400
Leukemia	MV411	0.0695	66.5	44.3	957	25.4[b]	72.6[b]	34.7	0.194
Ovarian	A2780	0.103	254	59.0	3660	23.8			0.216
	SKVO-3	0.0798	55.4	61.4	694	10.0			0.203
Breast	MB231	0.500 FIX	2.58	81.9	5.00		41.8	23.6	0.122
Pancreas	MIA PaCa-2	0.120	21.6	43.1	180		58.2	15.4	0.114

Model parameters are defined within the Methods and Materials section. RUV, residual unexplained variability.
[a] Correlation between inter-animal variability (IAV) λ_0 and IAV TV_0 of -90%. [b] Correlation between IAV λ_0 and IAV λ_1 of 100%

JPET Fast Forward. Published on April 24, 2018 as DOI: 10.1124/jpet.118.248286
This article has not been copyedited and formatted. The final version may differ from this version.

Figures

Figure 1

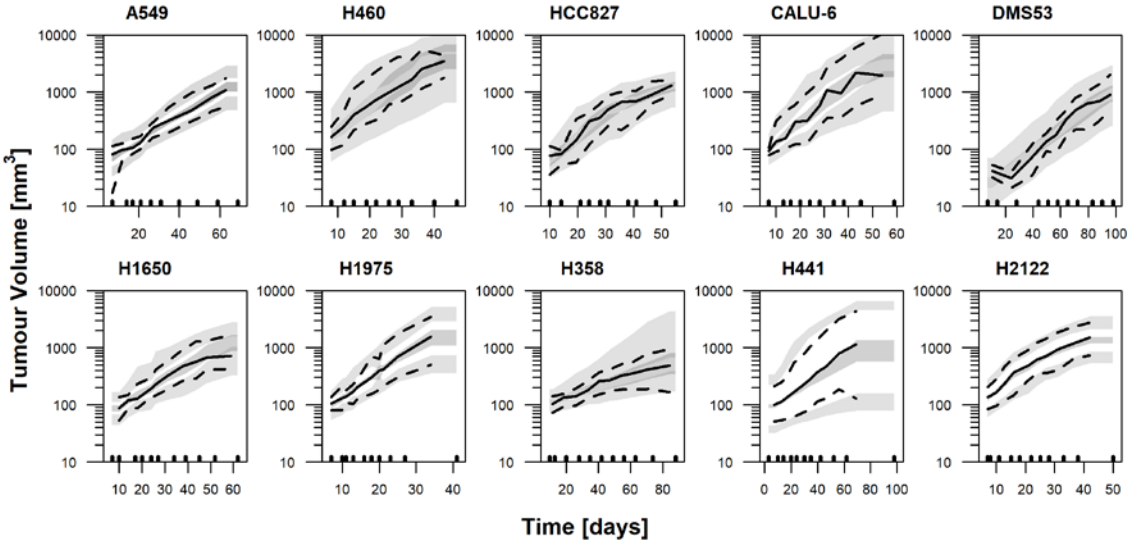

JPET Fast Forward. Published on April 24, 2018 as DOI: 10.1124/jpet.118.248286
This article has not been copyedited and formatted. The final version may differ from this version.

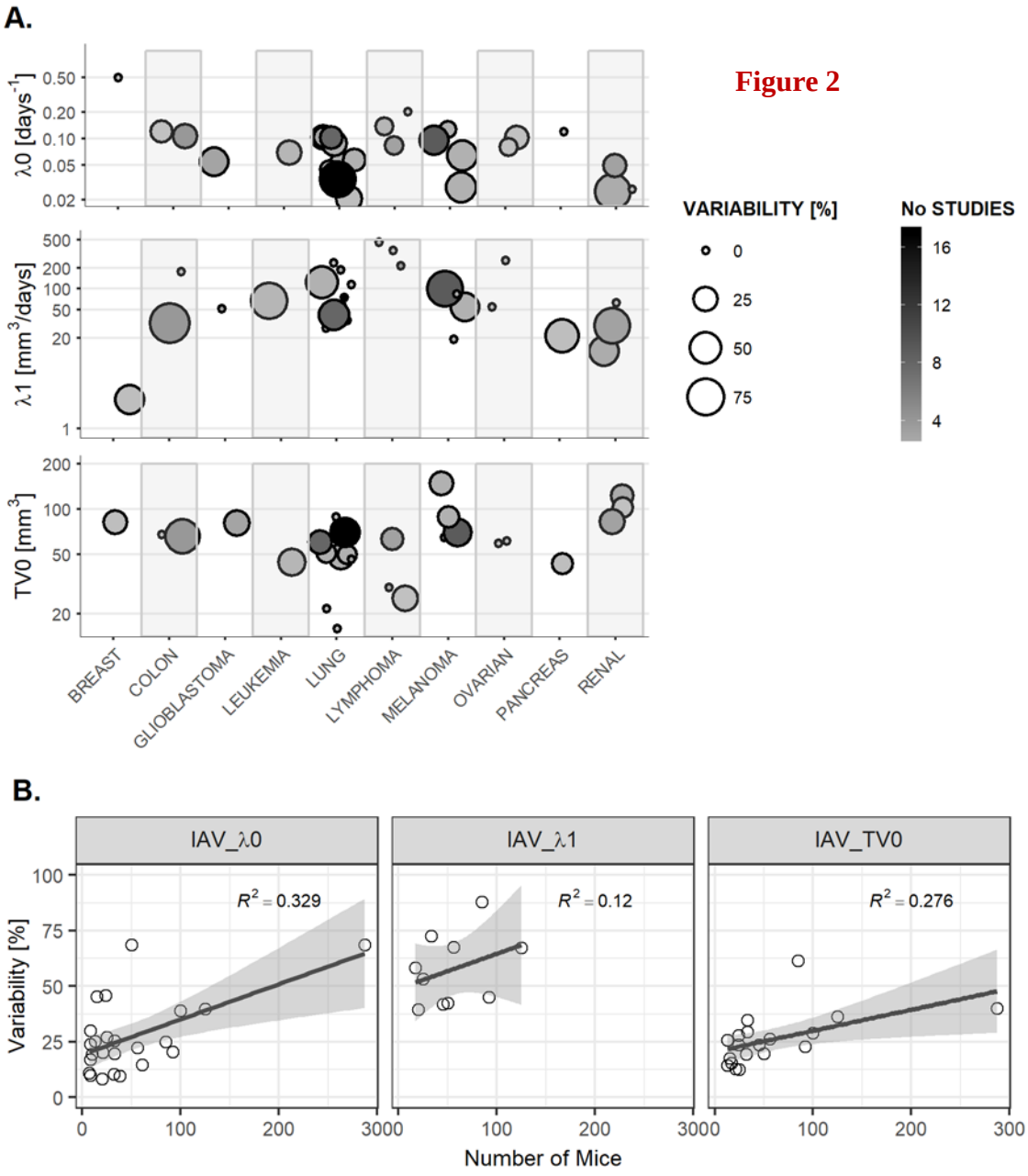

Figure 2

JPET Fast Forward. Published on April 24, 2018 as DOI: 10.1124/jpet.118.248286
This article has not been copyedited and formatted. The final version may differ from this version.

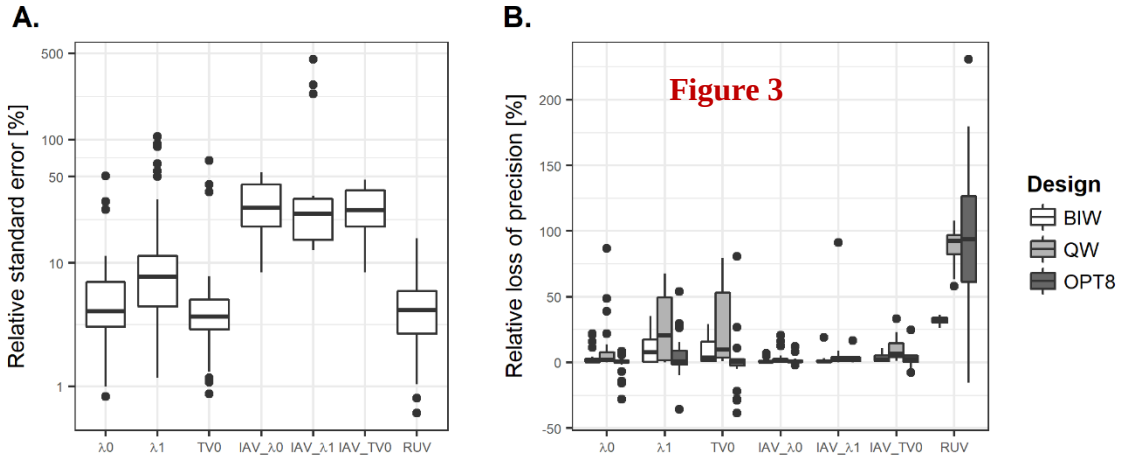

Figure 3

JPET Fast Forward. Published on April 24, 2018 as DOI: 10.1124/jpet.118.248286
This article has not been copyedited and formatted. The final version may differ from this version.

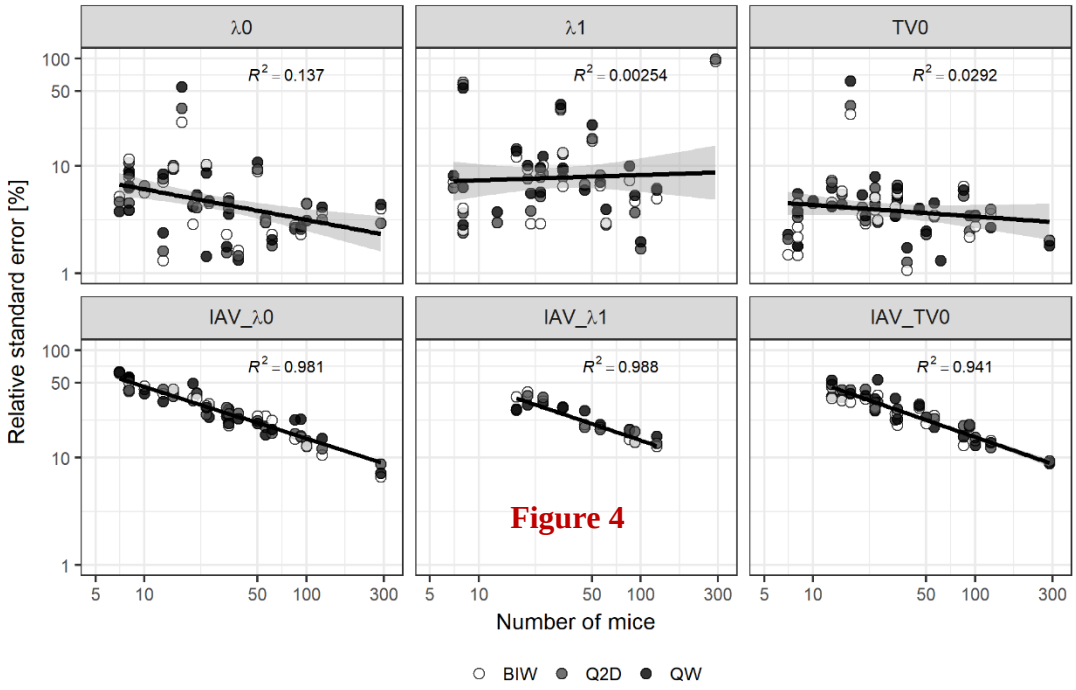

Figure 4

JPET Fast Forward. Published on April 24, 2018 as DOI: 10.1124/jpet.118.248286
This article has not been copyedited and formatted. The final version may differ from this version.

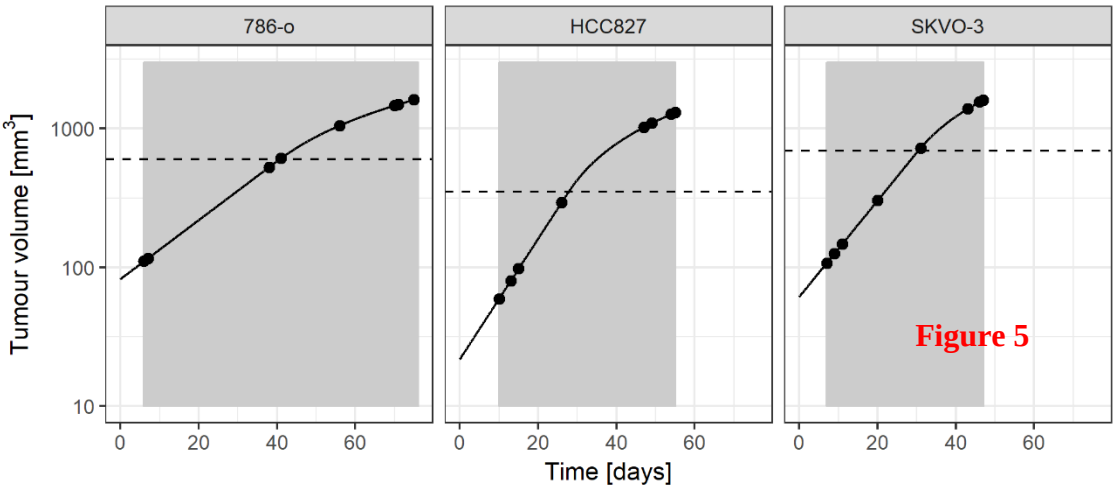

Figure 5